CHEMISTRY
A EUROPEAN JOURNAL

ChemPubSoc
Europe

DOI: 10.1002/chem.201203335

High-Efficiency Violet-Light-Emitting Materials Based on Phenanthro[9,10-*d*]imidazole

Zhao Gao,[a] Yulong Liu,[a] Zhiming Wang,[a, b] Fangzhong Shen,[a] He Liu,[a] Guannan Sun,[a] Liang Yao,[a] Ying Lv,[a] Ping Lu,*[a] and Yuguang Ma[a]

Highly efficient violet-light-emitting materials are of great importance owing to their wide applications in biology medical treatment,[1] sterilization,[2] and high-density information storage.[3] They can also be utilized to generate light of all colors, including blue, green, red, and white by energy-transfer processes in devices.[4–8] Moreover, the power consumption of a full-color display is highly dependent on the saturation degree of the violet-light-emitting material; that is, the higher saturation degree, the lower the power consumption.[9] The violet emission region locates in the lowest part of the CIE chromaticity diagram. Thus, material with a lower *y* coordinate value would give higher saturation degree because it would be closer to the spectral locus. The pursuit for efficient and stable violet-light-emitting material has been an ever-increasing issue in the field of organic optoelectronics. According to the European Broadcasting Union (EBU) standard blue CIE coordinate of (0.15, 0.06), there have been only a few reports on violet OLEDs that can match the emission with *y* coordinate lower than 0.06 with high efficiency.[10–18] One reason for the scarcity of reports is that it is difficult to simultaneously inject electrons and holes into such wide-band-gap organic semiconductors. The restriction in the π-conjugation length often causes a decrease in carrier injection and transport.[19,20] Herein, we report a new kind of violet-light-emitting materials M1 and M2, composed of phenanthro[9,10-*d*]imidazole (PI) and carbazole moieties. PI itself is a typical ultraviolet-light-emitting unit. PI also shows electron injection properties and good thermal stability based on our previous results,[21] which enables it to be an ideal unit for constructing stable, efficient violet-light-emitting material. After connecting with different amount of carbazoles, we found that M2 is a promising candidate for violet OLED with a high external efficiency of 3.02%, negligible efficiency roll-off, and good color stability. More importantly, the full width at half maximum (FWHM) of the EL emission is very narrow, which guarantees the violet emission color with CIE coordinate of (0.166, 0.056).

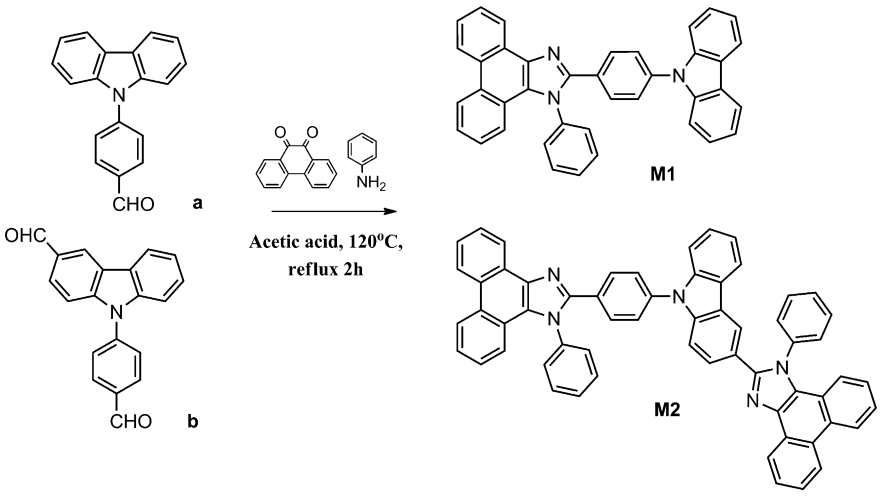

Scheme 1. Molecular structures of M1 and M2 and their synthesis from **a** and **b**, respectively.

Compounds M1 and M2 (Scheme 1) were synthesized in a facile manner by a one-pot reaction. PI derivatives with various structures can be conveniently built by simply tuning the aromatic aldehyde precursor involved. M1 and M2 were isolated with good yields (over 70%). They were characterized spectroscopically, and the datacorresponded well to their respective structures (Supporting Information).

[a] Dr. Z. Gao, Dr. Y. Liu, Dr. Z. Wang, Dr. F. Shen, Dr. H. Liu, G. Sun, Dr. L. Yao, Dr. Y. Lv, Prof. P. Lu, Prof. Y. Ma
State Key Laboratory of Supramolecular Structure and Materials
Jilin University, 2699 Qianjin Avenue
Changchun, 130012 (P. R. China)
Fax: (+86) 431-85193421
E-mail: lup@jlu.edu.cn

[b] Dr. Z. Wang
School of Petrochemical Engineering
Shenyang University of Technology
Liaoyang, 111003, (P. R. China)

Supporting information for this article is available on the WWW under http://dx.doi.org/10.1002/chem.201203335.

High thermal stabilities with decomposition temperatures (5% weight loss) of 406 °C and 515 °C for M1 and M2 were observed, as expected (Supporting Information, Figure S3 a). The glass transition temperature (T_g) of M1 was measured to be at 132 °C, and is accompanied with two cold crystallization peaks, indicating its crystallization trend at higher temperature. M2 showed a T_g of 207 °C without a crystallization peak, which was 75 °C higher than M1 because of the attachment of one more PI group (Supporting Information, Figure S3 b). Such a high T_g value and glass state implies that M2 could form morphologically stable films upon thermal evaporation, which is highly important for application in devices.[22,23] AFM characterization presented the similar results. M2 film fabricated by vacuum deposition exhibited a fairly smooth surface morphology with a roughness of 1.5 nm. After annealing at 120 °C for 0.5 h, the morphology became even better, with a roughness of only 0.59 nm (SI, Figure S4). In contrast, the surface of the M1 film showed a noticeable crystallization area, especially after annealing. The thermal properties and the film morphology of compounds have been significantly improved with the increased number of PI unit.

All of the compounds emit violet light in dilute THF solution (Figure 1). The emission peaks are at 381 nm and 399 nm for M1. As compared, M2 exhibits less than 10 nm

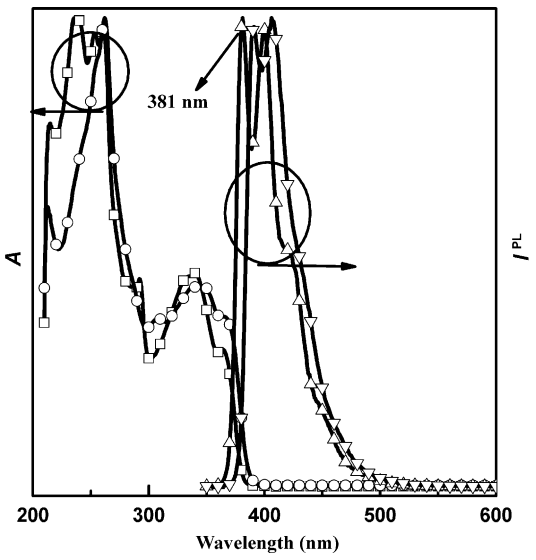

Figure 1. Normalized absorption (□, ○) and emission spectra (△, ▽) of M1 (□, △) and M2 (○, ▽) in THF. Concentration: 10^{-5} mol L^{-1}.

red-shift, peaking at 390 nm and 407 nm. It is noteworthy that both materials exhibit narrow emission with only 40 nm FWHM in the spectra. This is helpful for obtaining saturated color with a low *y* CIE coordinate in OLEDs. We also measured the fluorescence in different solvents with various polarities, and they all showed the similar emission spectra, implying that no intramolecular charge transfer existed in these compounds. In the film state (Supporting Information, Figure S5), the emission of these molecules showed red-shifts but were still located in the violet region. They exhibit similar absorption spectra (Figure 1). The maximum absorption peak at 262 nm is attributed to the isolated benzene ring connected with imidazole. The absorption band around 340 nm is attributed to the π–π* transition of phenanthro-[9,10-*d*]imidazole. The bandgap of M1 and M2 are calculated to be 3.24 and 3.18 eV according to their absorption edge in the film state. The data were summarized in Table 1.

Table 1. The photophysical data of M1 and M2.

	$\lambda^{abs}{}_{max}$ [nm][a] in THF	$\lambda^{PL}{}_{max}$ [nm][a] in THF	$\lambda^{abs}{}_{max}$ [nm] in film	$\lambda^{PL}{}_{max}$ [nm] in film	ΔE_g[b] [eV]	Φ_{fl}[c]
M1	266339	381399	260347	414	3.24	0.65
M2	262346	390407	268366	407	3.18	0.59

[a] The absorption and fluorescence spectra were measured in THF solution at a concentration of 1×10^{-5} mol L^{-1}. [b] Measured by the absorption edge of the thin film. [c] The solid-state quantum yield on the quartz plate using an integrating sphere apparatus.

HOMO and LUMO levels were measured by cyclic voltammetry using a glassy carbon disk (diameter 3 mm) as the working electrode, a platinum wire as the auxiliary electrode with a porous ceramic wick, and Ag/Ag^+ as the reference electrode. M1 exhibited one quasi-reversible oxidation wave with an onset potential of 0.94 V, which gave a HOMO level of −5.52 eV by comparison to ferrocene ($E_{HOMO} = -(eE_{ox}+4.58)$ eV). Calculated by the same method, M2 gave a HOMO level of −5.35 eV, which was 0.17 eV higher than M1, resulting in its easier injection of holes (Table 2; Supporting Information, Figure S6).

Table 2. The thermal and electrochemistry data of M1 and M2.

	T_g [°C]	T_d[a] [°C]	HOMO[b] [eV]	LUMO[b] [eV]	ΔE_g [eV]
M1	132	405	−5.52	−2.33	3.19
M2	207	515	−5.35	−2.22	3.13

[a] The temperature for 10% weight loss of the materials. [b] Calculated by comparing with ferrocene (Fc) and calibrated using $E_{1/2}(Fe/Fe^+) = 0.22$ V.

For a better understanding of the effect of the structural change on the energy levels and the carrier injection and transport ability, the hole-only and the electron-only devices of M1 and M2 were fabricated. The configuration of the hole-only device was ITO/PEDOT/M1 or M2 (80 nm)/Au, and the electron-only device had the configuration of ITO/TPBi (20 nm)/M1 or M2 (100 nm)/LiF/Al. The results (Figure 2) indicated that both M1 and M2 showed balanced carrier injection properties. Furthermore, both the electron and hole current values of M2 were higher than M1, indicating that more carriers could be transported to the emitting layer of M2 in OLED, which is crucial to obtain high efficiency owing to the dual-injection/transportation procedure of OLEDs. After the comprehensive characterization of M1 and M2, M2 shows an overall enhanced performance compared to M1, indicating that the introduction of one more

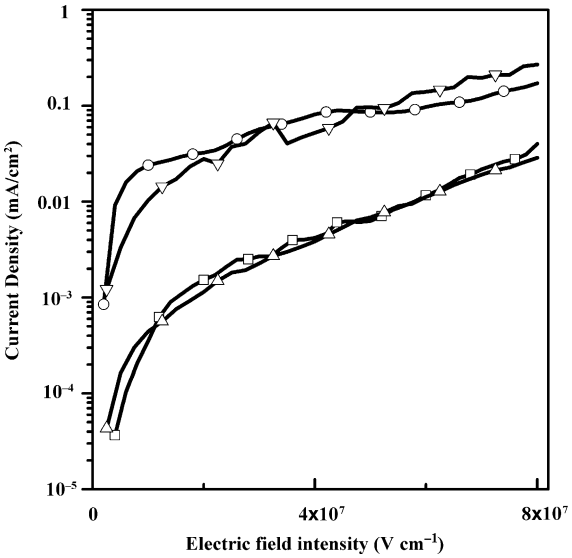

Figure 2. The electron (□, ○) and hole (△, ▽) current density versus electric field intensity curves of the single carrier devices based on M1 (□, △) and M2 (○, ▽).

PI unit helps to give a higher T_g, better film stability, more balanced carrier injection properties, and appropriate HOMO and LUMO levels.

Non-doped devices with a typical three-layer structure of ITO/NPB (80 nm)/M (30 nm)/TPBI (50 nm)/LiF (0.5 nm)/Al (100 nm) were fabricated with respect to their appropriate energy levels to investigate the potential applications of compounds in violet OLEDs. The devices of M1 and M2 both exhibit violet emission with a peak centered at 420 nm and 428 nm (Figure 3). The EL emission spectra of them show very narrow distribution, and the FWHM for them is only 40 nm, which is very helpful for obtaining saturated color. Thus, the CIE coordinates of (0.165, 0.050) for M1 and (0.166, 0.056) for M2 are obtained. This result is a good match with the requirement of EBU standard blue CIE coordinate of (0.15, 0.06), and it is among the very few compounds with a *y* coordinate lower than 0.06. Significantly, at voltages from 5 V to 10 V the spectra of both devices are kept unchanged and the CIE coordinates are almost identical, which show very good color stability for non-doped violet light-emitting diodes.

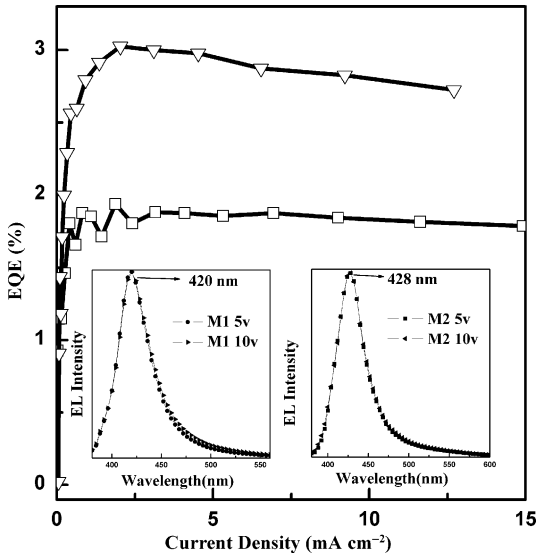

Figure 3. The external quantum efficiency versus current density curves of M1 (□) and M2 (▽). Inset: EL emission of M1 and M2 at different voltages.

The device performance of M1 and M2 is summarized in Table 3. A maximum external quantum efficiency (EQE) of 1.94% was obtained for M1, with a luminance efficiency (LE) of 0.65 cd A^{-1} and a power efficiency (PE) of 0.48 Lm W^{-1}. The device utilizing M2 as emission layer shows enhanced maximum EQE of 3.02% at a current density of 2.03 mA cm^{-2} with a LE of 1.53 cd A^{-1} and a PE of 0.86 Lm W^{-1} (Table 3). M1 and M2 show very low roll-off of the external efficiencies. Along with the increased number of PI group, the EL performance has been significantly improved, which is in correspondence with the comprehensive characterization results obtained above.

Table 3. Summary of the device performance of M1 and M2.

	LE_{max} [cd A^{-1}][a]	PE_{max} [lm W^{-1}][b]	B_{max} [cd m^{-12}][c]	EQE [%][d]	CIE (x, y)[e]
M1	0.65	0.48	3322	1.94	(0.165, 0.050)
M2	1.53	0.86	4329	3.02	(0.166, 0.056)

[a] The maximum values of luminance (LE_{max}). [b] The power efficiency (PE_{max}). [c] The maximum brightness (B_{max}). [d] External quantum efficiency (EQE). [e] Taken at 8 V.

In summary, we have designed a novel series of violet-light-emitting materials, M1 and M2, consisting of covalently bonded carbazole and phenanthroimidazole moieties. M2 exhibits a glass transition temperature T_g of 207 °C, good film stability, and balanced carrier injection properties. It is a non-doped device with a violet CIE of (0.166, 0.056), and an EQE of 3.02% was obtained. The FWHM of the EL emission is only 40 nm, which guaranteed the low *y* coordinate and saturated emission color. The color purity and the efficiency are among the best results ever reported for non-doped violet light-emitting diodes. This result gives us an inspiring basis for violet-light material design.

Experimental Section

(2-(4-(9H-carbazol-9-yl)phenyl)-1-phenyl-1H-phenanthro[9,10-*d*]imidazole (M1): A mixture of 4-(9H-carbazol-9-yl)benzaldehyde (1 g, 3.7 mmol), phenanthrene-9,10-dione (767.5 mg, 3.7 mmol), aniline (0.85 g, 18.5 mmol), ammonium acetate (1.14 g, 14.8 mmol), and acetic acid (10 mL) were refluxed under nitrogen in an oil bath. After 2 h, the mixture was cooled and filtered. The solid product was washed with an acetic acid/water mixture (1:1, 150 mL) and water. It was then purified by chromatography using CH_2Cl_2/petroleum ether (1:1) as an eluent to obtain the product as white powder. Yield: 75%. ^{1}H NMR (500 MHz,

DMSO, Hz): 8.96 (d, J = 8.30 Hz, 1H), 8.91 (d, J = 8.45 Hz, 1H), 8.74 (d, J = 7.36 Hz, 1H), 8.26 (d, J = 7.83 Hz, 2H), 7.89 (d, J = 8.22 Hz, 2H), 7.84–7.76 (m, 6H), 7.73 (t, J = 7.50 Hz, 6.43 Hz, 1H), 7.66 (d, J = 7.94 Hz, 2H), 7.59 (t, J = 6.97 Hz, 7.68 Hz, 1H), 7.46 (t, J = 7.50 Hz, 7.14 Hz, 2H), 7.40 (d, J = 8.61 Hz, 2H), 7.38 (t, J = 7.68 Hz, 7.68 Hz, 1H), 7.32 (t, J = 7.68 Hz, 7.68 Hz, 2H), 7.11 (d, J = 8.47 Hz, 1H); ^{13}C NMR (500 MHz, $CDCl_3$, Hz): 140.53, 130.80, 130.40, 130.14, 129.15, 128.39, 127.42, 126.61, 126.39, 126.02, 124.19, 123.57, 123.18, 120.91, 120.35, 120.20, 109.78; FTIR (KBr, ν, cm^{-1}) 3058, 1625, 1532, 1475, 1451, 1429, 1378, 1358, 1241, 1225, 1174, 1147, 1111, 1018, 1004, 929, 844, 750, 724, 667, 620, 563, 535; MALDI-TOF (m/z): [M$^+$] calcd for $C_{39}H_{25}N_3$: 535.64; Found: 535.90. Anal. calcd for $C_{39}H_{25}N_3$: C 87.45, H 4.70, N 7.84; Found: C 87.45, H 4.66, N 8.03.

1-phenyl-2-(4-(3-(1-phenyl-1H-phenanthro[9,10-d]imidazol-2-yl)-9H-carbazol-9-yl)phenyl)-1H-phenanthro[9,10-*d*]imidazole (M2): A mixture of 9-(4-formylphenyl)-9H-carbazole-3-carbaldehyde (957.3 mg, 3.198 mmol), phenanthrene-9,10-dione (1.465 mg, 7.036 mmol), aniline (2.978 g), ammonium acetate (1.92 g, 26.3 mmol), and acetic acid (10 mL) were refluxed under nitrogen in an oil bath. After 2 h, the mixture was cooled and filtered. The solid product was washed with an acetic acid/water mixture (1:1, 150 mL) and water. It was then purified by chromatography using CH_2Cl_2 as an eluent to obtain the product as white powder. Yield: 71%. ^{1}H NMR (500 MHz, DMSO, Hz): 8.97–8.94 (m, 2H), 8.92–8.89 (m, 2H), 8.76–8.74 (m, 2H), 8.35 (s, 1H), 8.08 (d, J = 8.22 Hz, 1H), 7.90 (d, J = 8.95, 2H), 7.85–7.77 (m, 10H), 7.73–7.70 (m, 5H), 7.67 (t, J = 8.37 Hz, 2H), 7.60–7.55 (m, 2H), 7.49–7.46 (t, J = 7.59 Hz, 7.59 Hz, 1H), 7.41–7.32 (m, 5H), 7.16 (t, J = 8.37 Hz, 1H), 7.11 (d, J = 7.59 Hz, 1H); FTIR (KBr, ν, cm^{-1}) 3056, 1577, 1496, 1453, 1382, 1234, 1175, 1141, 1107, 1039, 886, 844, 817, 755, 725, 699, 617, 570, 534; MALDI-TOF (m/z): [M$^+$] calcd for $C_{60}H_{37}N_5$: 827.97; Found: 828.0. Anal. calcd for $C_{60}H_{37}N_5$: C 87.04, H 4.50, N 8.46; Found: C 87.30, H 4.46, N 8.28.

Acknowledgements

This work is financially supported by the National Science Foundation of China (Grant Nos. 21107050, 60906021, 51203091), the Ministry of Science and Technology of China (grant number: 2009CB623605), PCSIRT, and the Graduate Innovation Fund of Jilin University (Grant No. 20121044).

Keywords: imidazoles · light-emitting materials · OLEDs · phenanthroquinone · violet light

[1] S. Landgraf, *J. Biochem. Biophys. Methods* **2004**, *61*, 125–134.
[2] L. T. T. Nhung, H. Nagata, A. Takahashi, M. Aihara, T. Okamoto, T. Shimohata, K. Mawatari, M. Akutagawa, Y. Kinouchi, M. Haraguchi, *The Journal of Medical Investigation* **2012**, *59*, 53–58.
[3] H. van Santen, J. H. M. Neijzen, *Jpn. J. Appl. Phys. Part 1* **2003**, *42*, 1110–1112.
[4] A. Kraft, A. C. Grimsdale, A. B. Holmes, *Angew. Chem.* **1998**, *110*, 416–443; *Angew. Chem. Int. Ed.* **1998**, *37*, 402–428.
[5] a) M. T. Lee, C. H. Liao, C. H. Tsai, C. H. Chen, *Adv. Mater.* **2005**, *17*, 2493–2497; b) H. H. Chou, Y. H. Chen, H. P. H, W. H. Chang, C. H. Cheng, *Adv. Mater.* **2012**, *24*, 5867–5871.
[6] a) M. R. Zhu, Q. Wang, Y. Gu, X. S. Cao, C. Zhong, D. G. Ma, J. G. Qin, C. L. Yang, *J. Mater. Chem.* **2011**, *21*, 6409–6415; b) S. J. Lee, J. S. Park, K. J. Yoon, Y. I. Kim, S. H. Jin, S. K. Kang, Y. S. Gal, S. Kang, J. Y. Lee, J. W. Kang, S. H. Lee, H. D. Park, J. J. Kim, *Adv. Funct. Mater.* **2008**, *18*, 3922–3930.
[7] a) A. L. Fisher, K. E. Linton, K. T. Kamtekar, C. Pearson, M. R. Bryce, M. C. Petty, *Chem. Mater.* **2011**, *23*, 1640–1642; b) H. Y. Li, A. S. Batsanov, K. C. Moss, H. L. Vaughan, F. B. Dias, K. T. Kamtekar, M. R. Bryce, A. P. Monkman, *Chem. Commun.* **2010**, *46*, 4812–4814.
[8] L. Q. Shi, Z. Liu, G. F. Dong, L. Duan, Y. Qiu, J. Jia, W. Guo, D. Zhao, D. L. Cui, X. T. Tao, *Chem. Eur. J.* **2012**, *18*, 8092–8099.
[9] a) J. W. G. Hunt, *Measuring Color*, Ellis Horwood, Chichester, **1980**, ; b) Z. Q. Jiang, Z. Y. Liu, C. L. Yang, C. Zhong, J. G. Qin, G. Yu, Y. Q. Liu, *Adv. Funct. Mater.* **2009**, *19*, 3987–3995.
[10] S. L. Lin, L. H. Chan, R. H. Lee, M. Y. Yen, W. J. Kuo, C. T. Chen, R. J. Jeng, *Adv. Mater.* **2008**, *20*, 3947–3952.
[11] a) D. H. Yu, F. C. Zhao, Z. Zhang, C. M. Han, H. Xu, J. Li, D. G. Ma, P. F. Yan, *Chem. Commun.* **2012**, *48*, 6157–6159; b) Y. I. Park, J. H. Son, J. S. Kang, S. K. Kim, J. H. Lee, J. W. Park, *Chem. Commun.* **2008**, 2143–2145.
[12] C. Liu, Y. H. Li, Y. Y. Zhang, C. L. Yang, H. B. Wu, J. G. Qin, Y. Cao, *Chem. Eur. J.* **2012**, *18*, 6928–6934.
[13] C. C. Wu, Y. T. Lin, K. T. Wong, R. T. Chen, Y. Y. Chien, *Adv. Mater.* **2004**, *16*, 61–65.
[14] C. J. Tonzola, A. P. Kulkarni, A. P. Gifford, W. Kaminsky, S. A. Jenekhe, *Adv. Funct. Mater.* **2007**, *17*, 863–874.
[15] S. Tang, M. R. Liu, P. Lu, H. Xia, M. Li, Z. Q. Xie, F. Z. Shen, C. Gu, H. P. Wang, B. Yang, Y. G. Ma, *Adv. Funct. Mater.* **2007**, *17*, 2869–2877.
[16] Z. Q. Gao, Z. H. Li, P. F. Xia, M. S. Wong, K. W. Cheah, C. H. Chen, *Adv. Funct. Mater.* **2007**, *17*, 3194–3197.
[17] C. Poriel, J. J. Liang, J. Rault-Berthelot, F. Barriére, N. Cocherel, A. M. Z. Slawin, D. Horhant, M. Virboul, G. Alcaraz, N. Audebrand, L. Vignau, N. Huby, G. Wantz, L. Hirsch, *Chem. Eur. J.* **2007**, *13*, 10055–10069.
[18] M. Santra, H. Moon, M.-H. Park, T.-W. Lee, Y. K Kim, K. H. Ahn, *Chem. Eur. J.* **2012**, *18*, 9886–9893.
[19] R. J. Holmes, B. W. D′Andrade, S. R. Forrest, X. Ren, J. Li, M. E. Thompson, *Appl. Phys. Lett.* **2003**, *83*, 3818–3820.
[20] X. F. Ren, J. L. Li, R. J. Holmes, P. I. Djurovich, S. R. Forrest, M. E. Thompson, *Chem. Mater.* **2004**, *16*, 4743–4747.
[21] Z. M. Wang, P. Lu, S. M. Chen, Z. Gao, F. Z. Shen, W. S. Zhang, Y. X. Xu, H. S. Kwok, Y. G. Ma, *J. Mater. Chem.* **2011**, *21*, 5451–5456.
[22] S. Tokito, H. Tanaka, K. Noda, A. Okada, Y. Taga, *Appl. Phys. Lett.* **1997**, *70*, 1929–1931.
[23] Z. K. Chen, H. Meng, Y. H. Lai, W. Huang, *Macromolecules* **1999**, *32*, 4351–4358.

Received: September 18, 2012
Revised: December 3, 2012
Published online: January 7, 2013

